Catalysis Science & Technology

Accepted Manuscript

ROYAL SOCIETY OF CHEMISTRY

www.rsc.org/catalysis

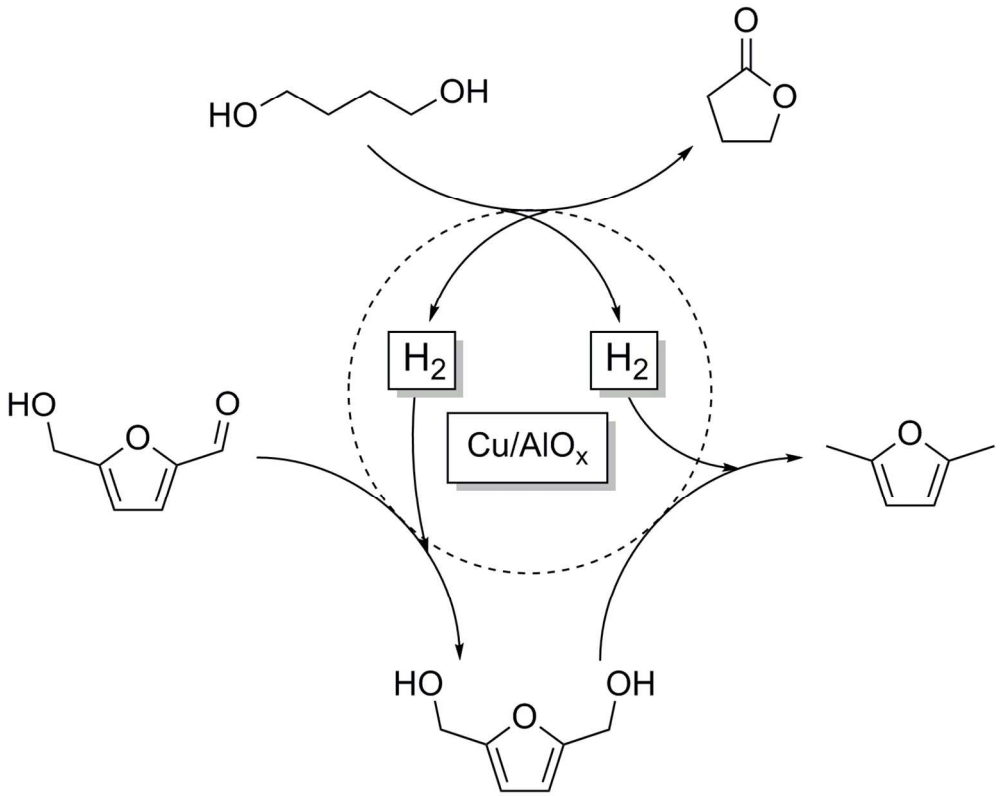

125x100mm (300 x 300 DPI)

Journal Name

RSCPublishing

ARTICLE

Combined 1,4-Butanediol Lactonization and Transfer Hydrogenation/Hydrogenolysis of Furfural-Derivatives under Continuous Flow Conditions

Christof Aellig,[a] Florian Jenny,[a] David Scholz,[a] Patrick Wolf,[a,b] Isabella Giovinazzo,[a] Fabian Kollhoff,[a] and Ive Hermans[a,b*]

Cite this: DOI: 10.1039/xoxxoooooox

Received ooth January 2012,
Accepted ooth January 2012

DOI: 10.1039/xoxxoooooox

www.rsc.org/

The oxygen-free lactonization of 1,4-butanediol to γ-butyrolactone, coupled to a sequential reductive-upgrading of furfural-derivatives following a transfer hydrogenation/hydrogenolysis mechanism was studied over AlO_x-supported copper catalysts. The Cu-Al-hydrotalcite-like catalyst-precursor was first reduced with H_2, forming dispersed Cu nanoparticles. The catalyst was characterized and tested for the dehydrogenation of various primary and secondary alcohols, optimizing the activation procedure and reaction conditions. Subsequently, the combined transfer-hydrogenation/hydrogenolysis to furfural-derivatives was investigated. All reactions were performed under continuous flow conditions to increase the space-time-yield and the selectivity towards the desired products, as well as to study the catalyst stability.

Introduction

A key challenge for the chemical industry is the replacement of the current oil-derived feedstocks with readily available and preferably renewable raw materials. Furfural and 5-(hydroxmethyl)furfural (HMF), available from the dehydration of biomass-derived sugars,[1] as shown in Scheme 1, are potential key platform-molecules in the manufacturing of value-added chemicals. 2,5-bis-(hydroxymethyl)furan (BHMF), obtained by hydrogenation of HMF, is, for instance, used as an intermediate in the production of polyurethane foams and polyesters.[2] Furfuryl alcohol (FA), the hydrogenation product of furfural, is widely used in the production of resins and as intermediate for various compounds such as vitamin C or lysine[3]. Further hydrogenolysis of FA and BHMF to methylfurane (MeF) and 2,5-dimethylfurane (DMeF) provides potential fuel substitutes which have more desirable properties than other bio-fuels such as ethanol.[4] Hydrogenation and hydrogenolysis of furfural has been extensively investigated with a variety of catalysts, including Ru[5a-5b], Pd[5c,5e,7] and Ir,[5d] but also promising noble metal-free and bimetallic catalysts,[5e-5i] based on Cu and Ni were reported. For the reductive upgrading of HMF, similar noble-metal catalysts have been used, including Au and Pt catalysts[5d,6].

Usually hydrogenation and hydrogenolysis reactions are performed under hydrogen pressure. In order to circumvent the inherent problems associated with H_2 (such as storage, safety and eco-efficiency), other hydrogen sources like 2-propanol,[5b,j,6b,8] formic acid[5d] or other alcohols[5k-l] have recently gained a lot of attention. In case of alcohols, low-cost carbonyl compounds (e.g. acetone) are formed that have to be disposed or used elsewhere. Using formic acid as a hydrogen donor, CO_2 is co-produced, making it less attractive.

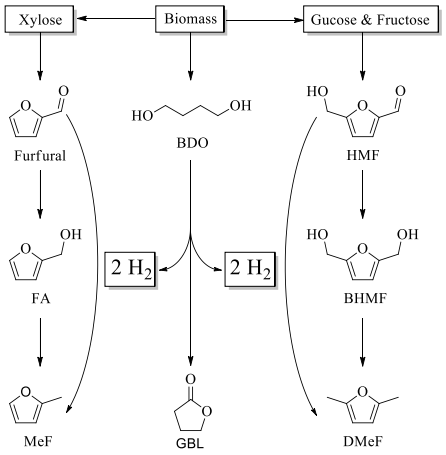

Scheme 1. Reductive upgrading of furfural and 5-(hydroxymethyl)furfural (HMF) to furfuryl alcohol (FA), 2,5-bis-(hydroxymethyl)furan (BHMF), 2-methylfurane (MeF) and 2,5-dimethylfurane (DMeF) via transfer hydrogenation/hydrogenolysis with parallel oxygen-free lactonization of 1,4-butanediol (BDO) to γ-butyrolactone (GBL).

For these reasons, one could envision improving reductive upgrading by selecting an appropriate renewable hydrogen source which would yield a valuable side-product. The oxygen-free 1,4-butanediol (BDO) lactonization to γ-butyrolactone (GBL), a useful intermediate in the synthesis of fine chemicals,[9b] produces two equivalents of molecular hydrogen. This makes BDO an excellent hydrogen source, readily available from fermentation of biomass.[7] In the past, the lactonization has been performed with various oxidants and catalysts,[9] including some Cu catalysts.[10] In addition, Mizugaki *et*

al.[11] reported that copper nanoparticles on AlO_x (Cu/AlO_x) derived from Cu-Al-hydrotalcite (Cu-Al-HT) show an excellent performance in the hydrogenolysis of glycerol to 1,2-propandiol. Prompted by these literature observations, we decided to investigate the transfer hydrogenation/hydrogenolysis using BDO as hydrogen-donor in the reductive upgrading of furfural and HMF with a Cu/AlO_x catalyst under continuous flow conditions.

Results and Discussion

Catalyst Synthesis and Activity

Various copper-containing materials were synthesized following a co-precipitation method as described in the experimental section. The catalyst composition was initially optimized in terms of activity and selectivity for the conversion of a BDO-furfural mixture by screening different supports (Al_2O_3, SiO_2 and Fe_2O_3) and Cu loadings (see tables S1 and S2 in the supporting information). The XRD pattern of the most promising Cu-Al-HT catalyst precursor is characteristic for hydrotalcite-like materials (Figures 1 and S1). The layered structure of the precursor could also be observed with electron microscopy (Figure S2). Reduction of the material in an H_2 flow ($T \geq 200$ °C) yielded copper nanoparticles on AlO_x, as evidenced by HAADF-STEM (Figures S3 and S5). The XRD pattern shows the formation of both Cu and Cu_2O phases (Figures 1 and S1). The XRD pattern of a catalyst exposed to H_2 (25 mL min^{-1}) at 250 °C for 4 hours does not show significant differences to the XRD pattern of a catalyst only reduced for 45 minutes (Figure S7). This indicates that the crystalline phases of the catalyst do not significantly change after 45 minutes of activation.

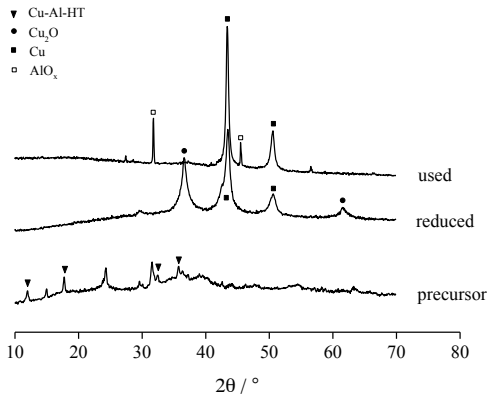

Figure 1. XRD pattern of Cu-Al-HT as prepared, the reduced catalyst (25 mL min^{-1} H_2, 45 min, 250 °C) and the catalyst exposed to reaction solution (c_{BDO}: 0.2 mol L^{-1}, $c_{furfural}$: 0.2 mol L^{-1}, *p*: 16 bar, *T*: 220 °C) for 6 hours.

Catalytic activity studies were performed in a continuous flow reactor (Scheme S1), offering several advantages over batch reactors, such as improved control of reaction parameters, enhanced heat- and mass-transfer, better mixing of the reactants, shorter reaction times and smaller reactor volumes.[12] Initial catalytic experiments focused on the oxygen-free dehydrogenation of alcohols. Although the reaction was performed at 16 bar over-pressure, H_2 gas bubbles were observed at the exit of the reactor. Therefore, the liquid hold ups were calculated with the correlation of Larachi *et al.*[13] for trickle bed reactors (see supporting information) in order to accurately determine contact times.

A significantly higher activity was observed if the catalyst was reduced at 250 instead of 200 °C (Figure S8). As Temperature Programmed Reduction (TPR) (Figure S9) reveals that the Cu^{2+}-to-Cu^0 reduction only starts at around 200 °C, this observation corroborates the working hypothesis that the active phase of the catalyst consists of dispersed copper nanoparticles. The dehydrogenation of various primary and secondary alcohols was investigated and the results are summarized in Table 1. In the case of benzyl alcohol and 2-heptanol, the catalyst did not only show activity in the dehydrogenation but also in the hydrogenolysis reaction, forming toluene and heptane, respectively. In the case of the conversion of BDO to GBL, the catalyst showed high activity and selectivity towards the desired lactone product (Figure 2). Small quantities of 3-hydroxy-tetrahydrofuran were detected by GC-MS, supporting the proposed reaction mechanism in Scheme 2.

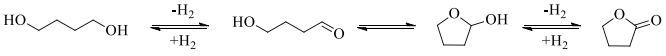

Scheme 2. Proposed mechanism for the oxygen-free lactonization of BDO to GBL.

Table 1. Oxygen-free dehydrogenation of different alcohols to their corresponding carbonyl compounds and lactonization of BDO to GBL.

Substrate	Product	Conversion / %[a]	Yield / %[a]
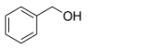		51	31[b]
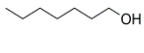	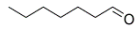	22	19
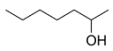	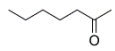	86	80[c]
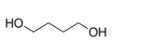		100	98

[a] Solvent: 1,4-dioxane, $c_{alcohol}$: 0.2 mol L^{-1} *p*: 16 bar, *T*: 220 °C, residence time: 2.7 min, activation *T*: 250 °C (25 mL min H_2 flow, 45 min). [b] Yield of toluene: 18 %. [c] Yield of heptane: 3 %.

We emphasize that no activity could be observed in blank experiments where the reactor was only filled with quartz particles or HT support (after thermal activation).

XRD analysis of a spent catalyst (6 hours on stream) reveals that the Cu_2O phase completely disappears and only elementary copper is left. Two additional peaks are appearing (Figures 1 and S1), indicating the formation of crystalline phases of alumina during the reaction.[14] Although there is a clear difference in activity (Figure S8), no significant difference in the diffractograms of the catalysts activated at 200 °C and 250 °C could be observed (Figures 1 and S1). However, there is a difference in the HAADF-STEM images after reaction. The catalyst that was activated at 250 °C showed clearly segregated Cu nanoparticles with an average particle size of 20-40 nm (Figure S6), whereas the catalyst that was activated at 200 °C shows a more disperse distribution with large particles of up to

60 nm (Figure S4). This difference in the structure of the catalyst probably explains the difference in reactivity (Figure S8). Further increase of the reduction temperature, however, leads to the formation of larger and less active particles.

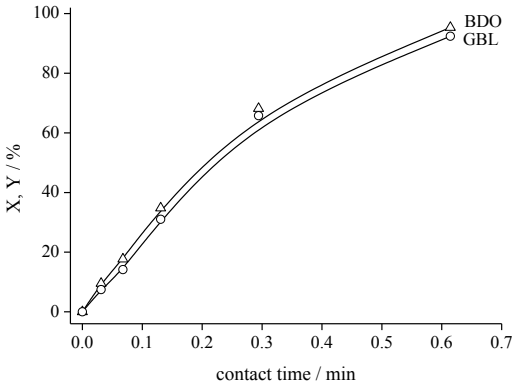

Figure 2. BDO conversion (X) and GBL yield (Y) against contact time (activation *T*: 250 °C (25 mL min^{-1} H_2 flow, 45 min), c_{BDO}: 0.2 mol L^{-1}, *p*: 16 bar, *T*: 220 °C).

Temperature Dependence and Mass-Transfer

The Arrhenius plots obtained in the temperature range 170 to 220 °C, and based on BDO consumption without acceptor or with benzaldehyde used as H-acceptor, show clear curvatures (Figure 3). This observation can point towards (i) mass-transfer limitations at higher temperatures, (ii) a change in the rate-determining step, or (iii) a rate-determining elementary reaction step which cannot be expressed by a simple power-law type model. In contrast, the Arrhenius plots using HMF and furfural as H-acceptors are perfectly linear (Figure 3), both giving an activation energy of 35 ± 1 kcal mol^{-1}, suggesting that the dehydrogenation of BDO to 4-hydroxy-*n*-butanal is the rate-determining step (RDS) (Scheme 2). This is confirmed by the fact that the reaction rate of both BDO and furfural consumption is first order in BDO (Figure S10). At reaction temperatures below 190 °C, the slopes associated with the pure BDO and the BDO-benzaldehyde transfer-hydrogenation system are linear, yielding the same activation energy of 35 ± 1 kcal mol^{-1} as the BDO-furfural and BDO-HMF systems. This leads to the assumption that in the 170 – 220 °C temperature range, the RDS is the same for all these systems.

Interestingly, at low reaction temperatures, the overall reaction rate is significantly lower for the BDO/furfural and BDO/HMF systems than for the BDO and BDO/benzaldehyde systems, despite our hypothesis of BDO dehydrogenation being the rate-determining step. One plausible explanation for this observation could be the strong adsorption of HMF and furfural to the catalyst, reducing the number of BDO-dehydrogenation sites, lowering the pre-exponential factor.

In order to test for external mass-transfer limitations (film diffusion), different reactor lengths were tested, adjusting the flow rate in a way that the residence time remains constant. According to film theory, the liquid film around the catalyst particle gets thinner with increasing flow rate. As a consequence, mass-transfer would be enhanced, resulting in an increase in conversion if this transfer were to be the controlling step. Changing the flow rate did however not significantly affect the conversion of both BDO and benzaldehyde (Figure 4). Therefore, external mass-transfer limitations can be excluded. On the other hand, the activation energy above 210 °C clearly drops below 10 kcal mol^{-1}. Since diffusion limitations could be excluded, the reaction mechanism is apparently more complex and cannot be expressed by a simple power-law-type model at higher temperatures. Further kinetic modeling is required to rationalize these observations.

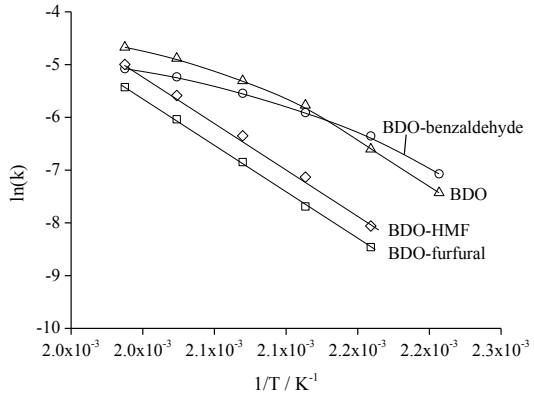

Figure 3. Arrhenius plot based on BDO consumption for pure BDO, BDO-benzaldehyde, BDO-HMF and BDO-furfural transfer hydrogenation systems (activation *T*: 250 °C (25 mL min^{-1} H_2 flow, 45 min), c_{BDO}: 0.2 mol L^{-1}, $c_{acceptor}$: 0.2 mol L^{-1}, *p*: 16 bar, *T*: 170 – 220 °C).

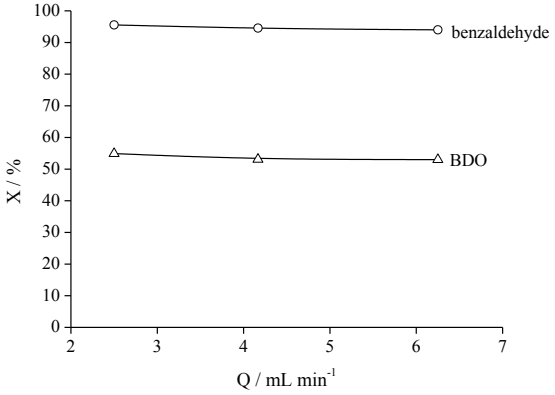

Figure 4. Conversion of BDO and benzaldehyde for different column lengths (6 cm, 10 cm and 15 cm) adjusting the flow rate to keep the residence time at 0.26 min (activation *T*: 250 °C (25 mL min^{-1} H_2 flow, 45 min), c_{BDO}: 0.2 mol L^{-1}, $c_{benzaldehyde}$: 0.2 mol L^{-1}, *p*: 16 bar, *T*: 220 °C).

The same test for external diffusion limitations was also performed with a BDO-furfural mixture at 220 °C (Figure S11) showing, as expected, no dependence of the conversion on the flow rate.

Catalyst Stability

In order to test the long-term stability of the catalyst, a reaction with a BDO-benzaldehyde mixture was performed at 220 °C over 24 h. Over the first 12 hours, a slight deactivation could be observed (*viz.,* a drop of 5% in the BDO conversion and 10 % for benzaldehyde; in

agreement with the reaction stoichiometry) as shown in Figure S14. After 12 hours, the catalytic performance remains constant and no further deactivation could be observed. Although several trends could explain the decrease in conversion over the first 12 hours, no evidence for significant copper leaching could be obtained from ICP-OES analysis after digestion of the catalyst. HAADF-STEM analysis reveals an increase in the particle size (from around 20 nm to 40 nm) of freshly activated catalyst at 250 °C and after 6 hours of reaction with BDO-furfural mixture (Figures S5 and S6). EDXS analysis (Figures S12 and S13) clearly shows that the carbon content on the support is significantly higher after reaction. Based on these observations, we propose that the main reason for the slight loss in activity should be attributed to sintering and coking of the catalyst. A 5 % increase in activity could be observed after air calcination of the used catalyst (after 24 h on stream) at 450 °C, followed by reactivation under H_2, indicating that coking is indeed (partially) contributing to deactivation. Although no significant Cu leaching could be observed in the present system, we emphasize that real biomass streams may contain residual water from previous processing, and that leaching of Cu could become an issue.[15]

Transfer Hydrogenation/Hydrogenolysis of Furfural and HMF

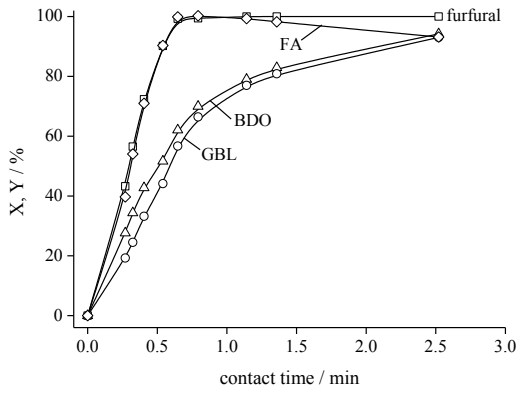

Figure 5. Conversion of BDO to GBL and furfural to FA (activation *T*: 240 °C (25 mL min^{-1} H_2 flow, 45 min), c_{BDO}: 0.2 mol L^{-1}, $c_{furfural}$: 0.2 mol L^{-1}, *p*: 16 bar, *T*: 220 °C).

The hydrogenation of furfural with BDO yielded 99 % FA and 57 % GBL at a residence time of 0.65 minutes under continuous flow conditions (Figure 5). One can clearly see that FA is decreasing at residence times higher than 0.5 min, due to hydrogenolysis to MeF and other side-reactions like decarbonylation and ring hydrogenation. The by-products furan, THF and 2-methyl-tetrahydrofuran were detected by GC-MS. Because of the low selectivity towards the desired MeF product, more focus was put on the selective conversion of furfural to FA and of BDO to GBL, respectively (Figure 5). When stoichiometric amounts of BDO (0.1 mol L^{-1} instead of 0.2 mol L^{-1}) were used in combination with furfural (0.2 mol L^{-1}), only 81 % yield of FA could be obtained at 100 % BDO conversion.

The transfer hydrogenation/hydrogenolysis of HMF proceeds mainly *via* BHMF, which, subsequently, undergoes hydrogenolysis *via* 2-methyl-furfuryl alcohol (MFA) to DMeF. Traces of 2-methyl-furfural (MeFF) could be observed at low residence times using GC-MS. At higher residence times, traces of 2,5-dimethyltetrahydrofuran could be detected.

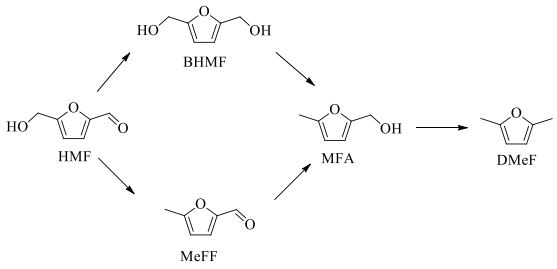

Scheme 3. Reaction network for the transfer hydrogenation/hydrogenolysis of HMF to BHMF and DMeF.

At a residence time of 0.6 minutes the hydrogenation of HMF yields 93 % BHMF and 28 % GBL at conversions of 94 % and 29 % for HMF and BDO, respectively. HMF deoxygenation results in 72 % yield of DMF at 100 % HMF and BDO conversion and 99 % GBL yield after 29 minutes (Figure 6).

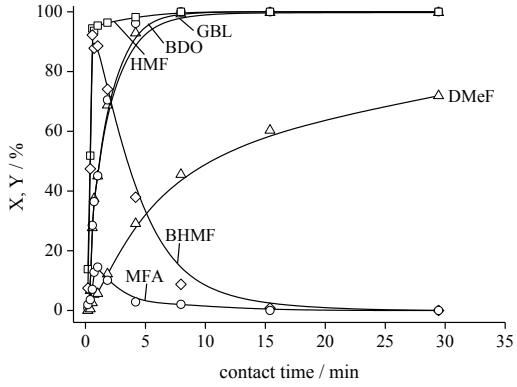

Figure 6. Conversion of BDO to GBL and HMF to BHMF and DMF (activation *T*: 250 °C (25 mL min^{-1} H_2 flow, 45 min), c_{BDO}: 0.6 mol L^{-1}, c_{HMF}: 0.2 mol L^{-1}, *p*: 16 bar, *T*: 220 °C).

Conclusions

The high oxygen content of biomass-derived platform molecules asks for efficient methods for the reductive upgrading to chemicals and fuels. After activation of a Cu-Al-HT-like precursor with H_2 at temperatures above 200 °C, Cu nanoparticles dispersed on AlO_x are formed. The present catalyst is active not only in the oxygen-free dehydrogenation of alcohols to their corresponding carbonyl compounds, but also for the oxygen-free lactonization of BDO to GBL with parallel hydrogenation/hydrogenolysis of furfural or HMF. The use of 1,4-butanediol as hydrogen donor has several advantages: (i) it can be obtained by fermentation, (ii) it releases two equivalents H_2, and (iii) the product GBL has many applications and can be further used in the chemical value-chain. Depending on the residence time, FA can be obtained with a yield of 99 %. At longer residence times, MeF and other ring-hydrogenation and decarbonylation products are formed. In case of HMF, BHMF can be obtained with 93 % yield at a residence time of 0.6 min. The

subsequent hydrogenolysis of BHMF yields 72 % DMeF after 29 minutes contact time.
The stability of the catalyst was tested over 24 hours showing that the conversion of both BDO and benzaldehyde slightly decreases over the first 12 hours, thereafter remaining stable. The reason for the deactivation can at least partially be attributed to sintering and coking.

Experimental Section

Quantification of furfural (Sigma-Aldrich, 99%), FA (Aldrich, 98%), HMF (Aldrich, ≥99%), BHMF, DMeF (TCI, >98%), BDO (ABCR, 99%) and GBL (Acros, 99%) was done with dodecane (Acros, 99%) as internal standard and benzaldehyde (Acros, >98%), benzyl alcohol (Acros, 99%), heptanal (ABCR, 97%), 1-heptanol (ABCR, 99%), 2-heptanone (ABCR, 99%) and 2-heptanol (Acros, >99%) with biphenyl (Acros, 99%) as internal standard on a GC-FID with HP-FFAP column. 1,4-dioxane (Fluka, ≥99.5%) was used as solvent in all experiments.

Synthesis of BHMF

To a solution of HMF (Aldrich-Fine Chemicals, 99 %; 2.02 g, 16 mmol) in dry methanol (ABCR-Chemicals, 99.9; 16 mL), $NaBH_4$ (1.21 g, 32 mmol) was slowly added at 273 K under constant stirring. After addition of the reductant, the ice bath was removed and the solution was stirred at room temperature for an additional 15 min. The reaction was quenched with 4 mL deionized water and 5 mL HCl (2 M). The product was extracted 7 times with 10 mL ethyl acetate and subsequently dried over $MgSO_4$. After filtration the solvent was removed under reduced pressure yielding solid BHMF (0.65 g, 55%).

Synthesis of Cu-Al-HT

A solution of $Cu(NO_3)_2{\cdot}3H_2O$ (Aldrich-Fine Chemicals, 99 %; 6.04 g, 25 mmol) and $Al(NO_3)_3{\cdot}9H_2O$ (Aldrich-Fine Chemicals, 99 %; 4.96 g, 13.2 mmol) in deionized water (35 mL) and Na_2CO_3 (Acros Organics, 99.6; 2.98 g, 28 mmol) in deionized water (30 mL) were added drop-wise simultaneously to 50 ml of deionized water in a beaker under vigorous stirring and the pH was kept constant at 8-9 by adding NaOH (12 g, 0.3 mol) in deionized water (100 mL). The resulting pale blue slurry was transferred into a round-bottom flask and aged at 65 °C for two hours. The product was filtrated and washed thoroughly with deionized water and dried at 65 °C in a vacuum oven for 16 hours. Reduced Cu-loadings were achieved by reducing the amount of $Cu(NO_3)_2{\cdot}3H_2O$ to 0.5 and 0.25, respectively, of the initial amount.

Synthesis of Cu/Fe_2O_3

Cu/Fe_2O_3 was prepared according to the above mentioned procedure by replacing $Al(NO_3)_3{\cdot}9H_2O$ with the corresponding amount of $Fe(NO_3)_3{\cdot}9H_2O$ (Merck, ≥98%).

Synthesis of Cu/SiO_2

Cu/SiO_2 was prepared according to a literature procedure.[16] An aqueous solution of NaOH (4 M) was added dropwise to a solution of $Cu(NO_3)_2{\cdot}3H_2O$ (11.66 g, 48.3 mmol) under vigorous stirring. To the resulting slurry 5.29 g of a colloidal silica solution (30% SiO_2 in water, Aldrich) was added. The gel was aged at 65°C for two hours. After filtration the product was washed thoroughly with deionized water and dried in a vacuum oven at 65°C for 16 hours.

Continuous flow experiments

A tubular reactor (Ø 4.6 mm, Scheme S1) was packed with a mixture (void fraction 0.35) of Cu-Al-HT (1.5 g) diluted with quartz (0.9 g; Ø 0.1-0.2 mm) and attached to a pre-column (Ø 4.6 mm, length: 10 cm) filled with glass spheres (Ø 0.8 mm). The inlet of the reactor was connected to an HPLC pump; the outlet to a back-pressure regulator. The catalyst was pretreated at 250 °C or 200 °C, ambient pressure, under constant H_2-flow (25 ml min^{-1}) for 45 min. Prior to pumping the reaction solvent over the catalyst bed the pressure was increased to 16 bar H_2 pressure with the use of the back-pressure regulator. Before starting the reaction, the H_2-line was closed and the pressure was kept at 16 bar to prevent evaporation of the solvent.

Catalyst characterization

The copper contents in untreated, reduced and used catalysts were determined by ICP-OES (HORIBA Ultra 2). Reduced catalyst was prepared according to the pretreatment procedure described above. For ICP-OES measurements all samples were calcined in air at 600°C for 5 hours and dissolved in aqua regia (37% HCl : 65% HNO_3, 3:1). The copper contents were determined as: 65.6 wt% (untreated), 62.6 wt% (reduced at 200 °C), 55.3 wt% (reduced at 250 °C). Powder X-ray diffraction measurements were conducted on a PANalytical X'Pert Pro-MPD (CuKα radiation, X'Celerator linear detector system, 2θ=10-70°, step size of 0.033°, ambient conditions). TEM-images of untreated and STEM-images of reduced and used catalysts were recorded on a Hitachi HD2700CS STEM (aberration-corrected dedicated STEM, cold field-emission source, 200 kV). H_2-TPR of untreated Cu-Al-HT was performed on a THERMO TPDRO 1100.

Acknowledgements

Financial support from the Swiss National Science Foundation (SNSF; project 200021_146661) is gratefully acknowledged. The authors also thank Dr. Frank Krumeich for his help with the electron microscopy.

Notes and references

[a] ETH Zurich, Institute for Chemical and Bioengineering, Wolfgang-Pauli-Strasse 10, 8093 Zurich (Switzerland)
b current address: University of Wisconsin – Madison, Department of Chemistry & Department of Chemical and Biological Engineering, 1101 University Ave, Madison WI 53706 (USA)
Email: hermans@chem.wisc.edu
Electronic Supplementary Information (ESI) available: catalyst screening, (S)TEM images, TPR profile and liquid hold-up calculations. See DOI: 10.1039/b000000x/

1 a) A. S. Mamman, J. M. Lee, Y. C. Kim, I. T. Hwang, N. J. Park, Y. K. Hwang, J. S. Chang, J. S. Hwang, *Biofuels, Bioprod. Biorefin.*, 2008, **2**, 438; b) C. Aellig, I. Hermans, *ChemSusChem*, 2012, **5**, 1737
2 W. J. Pentz, *GB Patent 2131014*, **1984**.

3 A. Corma, S. Iborra, A. Velty, *Chem. Rev.*, 2007, **107**, 2411.
4 W. Chongming, X. Hongming, D. Ritchie, G. Akbar, M. H. Jose, S. Shijin, M. Xiao, *Fuel*, 2013, **103**, 200.
5 a) A. S. Gowda, S. Parkin, F. T. Lapido, *Appl. Organometal. Chem.*, 2012, **26**, 86; b) Z. Strassberger, M. Mooijman, E. Ruijter, A. H. Alberts, C. de Graaf, R. V. A. Orru, G. Rothenberg, *Appl. Organometal. Chem.*, 2010, **24**, 142; c) J. G. Stevens, R. A. Bourne, M. V. Twigg, M. Poliakoff, *Angew. Chem.*, 2010, **122**, 9040; d) T. Thananatthanachon, T. B. Rauchfuss, *ChemSusChem*, 2010, **3**, 1139; e) S. Sitthisa, D. E. Resasco, *Catal. Lett.*, 2011, **141**, 784; f) M. M. Villaverde, N. M. Bertero, T. F. Garetto, A. J. Marchi, *Catalysis Today*, 2013, **213**, 87; g) X.-Y. Hao, W. Zhou, J.-W. Wang, Y.-Q. Zhang, S. Liu, *Chemistry Letters,* 2005, **34**, 1000; h) K. Yan, J. Liao, X. Wu, X. Xie, *RSC Adv.*, 2013, **3**, 3853; i) H. Luo, H. Li, L. Zhuang, *Chemistry Letters*, 2001, 404; j) M. Chia, J. A. Dumesic, *Chem. Comm.*, 2011, **47**, 12233; k) L. Bui, H. Luo, W. R. Gunther, Y. Román-Leshkov, *Angew. Chem. Int. Ed.*, 2013, **52**, 8022; l) K. Barta, T. D. Matson, M. L. Fettig, S. L. Scott, A. V. Iretskii, P. C. Ford, *Green Chem.*, 2010, **12**, 1640.
6 a) J. Ohyama, A. Esaki, Y. Yamamoto, S. Aral, A. Satsuma, *RSC Adv.*, 2013, **3** 1033; b) M. Balakrishnan, E. R. Sada, A. T. Bell, *Green Chem.*, 2012, **14**, 1626; c) T. Thananatthanachon, T. B. Rauchfuss, *Angew. Chem. Int. Ed.*, 2010, **49**, 6616; d) J. Jae, W. Zheng, R. F. Lobo, D. G. Vlachos, *ChemSusChem*, 2013, **6**, 1158.
7 H. Yim, R. Haselbeck, W. Niu, C. Pujol-Baxley, A. Burgard, J. Boldt, J. Khandurina, J. D. Trawick, R. E. Osterhout, R. Stephen, J. Estadilla, S. Teisan, H. B. Schreyer, S. Andrae, T. H. Yang, S. Y. Lee, M. J. Burk, S. Van Dien, *Nat. Chem. Biol.*, 2011, **7**, 445.
8 a) D. Scholz, C. Aellig, I. Hermans, *ChemSusChem*, 2014, **7**, 268; b) X. Wang, R. Rinaldi, *Energy Environ. Sci.*, 2012, **5**, 8244.
9 a) X. Li, Y. Cui, X. Yang, W.-L. Dai, K. Fan, *App. Catal. Gen.*, 2013, **458**, 63; b) J. Huang, W.-L. Dai, H. Li, K. Fan, *J. Catal.*, 2007, **252**, 69; c) T. Mitsudome, A. Noujima, T. Mizugaki, K. Jitsukawa, K. Kaneda, *Green Chem.*, 2009, **11**, 793; d) Y. Lin, X. Zhu, Y. Zhou, *J. Organometal. Chem.*, 1992, **429**, 269; e) T. Suzuki, K. Morita, M. Tsuchida, K. Hiroi, *Org. Lett.*, 2002, **4**, 2361; f) T. Baba, K. Kameta, S. Nishiyama, S. Tsuruya, M. Masai, *Bull. Chem. Soc. Jpn.*, 1990, **63**, 255; g) T. Baba, K. Kameta, S. Nishiyama, S. Tsuruya, M. Masai, *J. Chem. Soc., Chem. Commun.,* 1989, 1072-1073; h) Y. Endo, J.-E. Bäckvall, *Chem. Eur. J.*, 2011, **17**, 12596; i) W.-H. Kim, I. S. Park, J. Park, *Org. Lett.*, 2006, **8**, 2543; j) M. Ito, A. Osaku, A. Shiibashi, T. Ikariya, *Org. Lett.*, 2007, **9**, 1821; k) J. Zhang, E. Balaraman, G. Leitus, D. Milstein, *Organometallics*, 2011, **30**, 5716; l) A. Sølvhøj, R. Madsen, *Organometallics*, 2011, **30**, 6044; m) K.-N. T. Tseng, J. W. Kampf, N. K. Szymczak, *Organometallics*, 2013, **32**, 2046; n) M. C. Bagley, Z. Lin, D. J. Phillips, A. E. Graham, *Tetrahedron Lett.*, 2009, **50**, 6823; o) T. Morimoto, M. Hirano, K. Iwasaki, T. Ishikawa, *Chem. Lett.*, 1994, 53; p) D. V. Seleznev, L. N. Zorina, V. N. Trifonova, V. V. Zorin, D. L. Rakhmankulov, *Russ. J. Org. Chem.*, 2002, **38**, 1064; q) T. R. Beebe, R. Adkins, R. Baldridge, V. Hensley, D. McMillen, D. Morris, R. Noe, F. W. Ng, G. Powell, C. Spielberger, M. Stolte, *J. Org. Chem.*, 1985, **50**, 3015; r) S. Kondo, S. Kawasoe, H. Kunisada, Y. Yuki, *Synthetic Comm.*, 1995, **25**, 719; s) T. Miyazawa, T. Endo, *J. Org. Chem.*, 1985, **50**, 3931; t) H. Tanaka, Y. Kawakami, K. Goto, M. Kuroboshi, *Tetrahedron Lett.*, 2001, **42**, 445; u) Y. Ishii, T. Yoshida, K. Yamawaki, M. Ogawa, *J. Org. Chem.*, 1988, **53**, 5549; v) K. S. Kim, W. A. Szarek, *Carbohyd. Res.*, 1982, **104**, 328.
10 a) D. W. Hwang, P. Kashinathan, J. M. Lee, J. H. Lee, U. Lee, J.-S. Hwang, Y. K. Hwang, J.-S. Chang, *Green Chem.*, 2011, **13**, 1672; b) Y.-L. Zhu, H.-W. Xiang, G.-S. Wu, L. Bai, Y.-W. Li, *Chem. Commun.*, 2002, 254; c) Y. Mikami, K. Ebata, T. Mitsudome, T. Mizugaki, K. Jitsukawa, K. Kaneda, *Heterocycles*, 2010, **80**, 855.
11 T. Mizugaki, R. Arundhati, T. Mitsudome, K. Jitsukawa, K. Kaneda, *Chem. Lett.*, 2013, **42**, 729.
12 a) R. L. Hartman, J. P. McMullen, K. F. Jensen, *Angew. Chem.*, 2011, **123**, 7642; b) G. Jas, A. Kirschning, *Chem. Eur. J.*, 2003, **9**, 5708; c) A. Kirschning, W. Solodenko, K. Mennecke, *Chem. Eur. J.*, 2006, **12**, 5972.
13 V. V. Rande, R. Chaudhari, P. R. Gunjal, *Trickle Bed Reactors, Reactor Engineering & Applications*, Elsevier B.V., Oxford, 2011**.**
14 P. S. Santos, H. S. Santos, S. P. Toledo, *Mat. Res.*, 2000, **3**, 104.
15 A. M. Henge, C. V. Rode, *Green Chem.*, 2012, **14**, 1064.
16 Zhiwei Huang, Fang Cui, Haixiao Kang, Jing Chen, Xinzhi Zhang, Chungu Xia, *Chem. Mater.*, 2008, **20**, 5090.

